Utrecht University

Do salt diapirs promote the geothermal potential of shallow depth aquifers?

December 15, 2023

MSc thesis
Utrecht University
Department of Earth Sciences

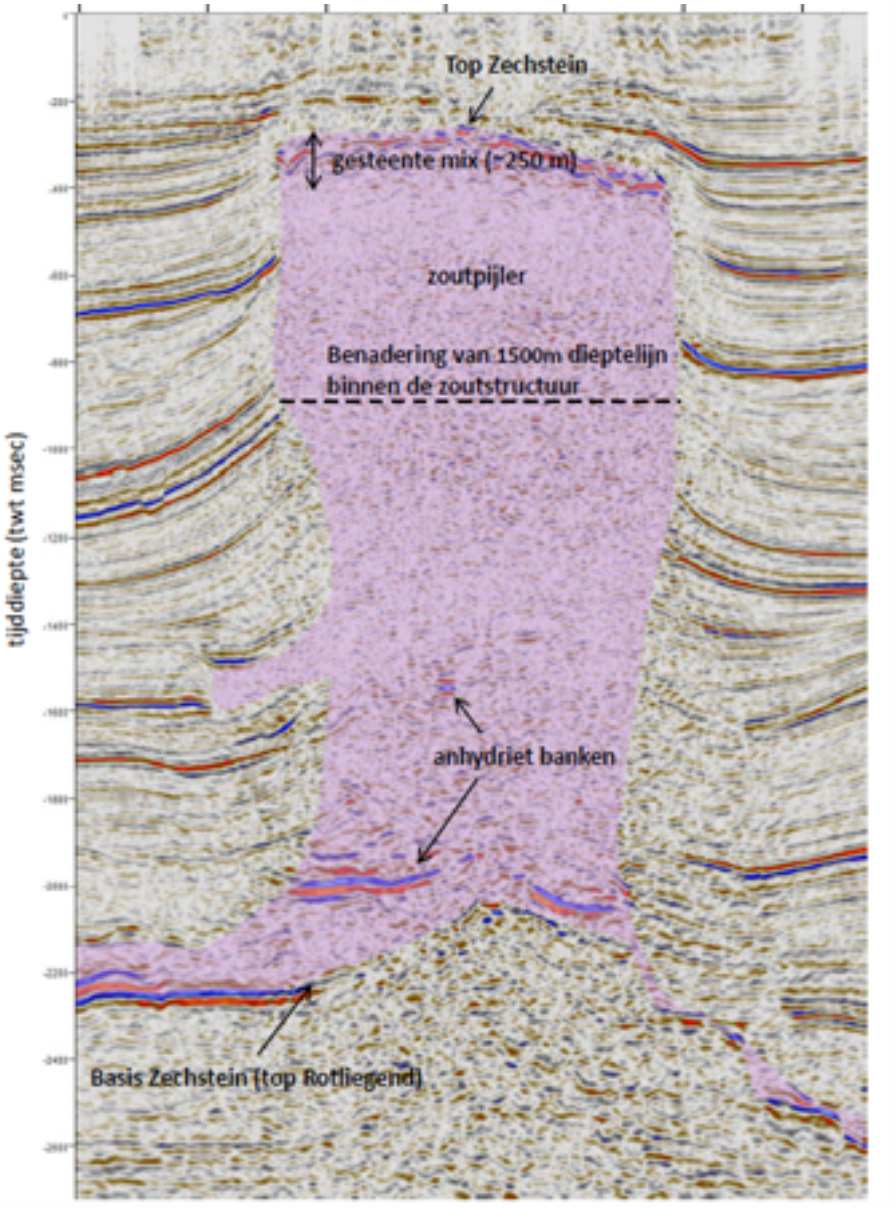

by

Michiel van den Berg
(Student number 6281761)

Thesis supervisors:
Fred Beekman (UU)
Hans Veldkamp (TNO)

Abstract

This study investigates the thermal behavior of the Onstwedde salt pillar (NE Netherlands) and its implications for geothermal energy exploration. By making a reinterpretation of the available seismic data, a new static 3D model of the Onstwedde salt pillar and its surroundings. Through the utilization of 3D modeling, the research consistently demonstrates a significant positive temperature anomaly up to 15-20 °C in and above the crest of the salt pillar. The modelling results are in line with temperature measurement from wells around a salt pillar in Germany. A glacier incision valley, situated above the pillar and filled with low conductivity course and fine sandstones, is shown to act as a thermal insulator, with a contribution of ca 5 °C to the predicted thermal anomaly. A parameter sensitivity study investigating different conductivity values and thermal boundary conditions and the role of the glacier valley shows variations of only a few degrees C in the predicted temperature anomaly, which therefore is considered to be robust.

The results of this study indicate that there is potential to exploit geothermal heat from the crest of the Onstwedde salt pillar. To confirm this, there is an urgent need for temperature measurements in exploration wells in and around shallow salt pillars. Uncertainties of the regional thermal boundary conditions and the influence of convection in surrounding rocks emphasize the need for further research to refine our understanding of these factors and optimize the potential of salt domes for sustainable energy extraction.

Contents

List of Figures

List of Tables

There is an increasing interest in the exploitation of geothermal energy as a replacement for fossil fuels (Daniilidis and Herber [3]). Geothermal energy, if developed economically, could become a cheap and green solution for the generation of direct heat. Geothermal closed loop systems already exist at deeper depths (Self et al. [17]), but at shallower depths it could also be an option. This is were salt-pillar like structures could play a role. Salt rocks, mainly halite, have a higher thermal conductivity at room temperature (6.5 W/m K, Hantschel and Kauerauf [4]) than other sedimentary rocks (1.6 W/m K for shale and 4.0 W/m K for sandstone Robertson [16]). Salt pillars could have a chimney like effect on the heat coming from the subsurface and causing the ground around the top of the salt pillar to be warmer than at locations further away from the salt pillar. This would mean that shallower wells can be drilled above salt pillars to reach the same temperature. And with drilling being the most expensive part of the process this would make drilling around salt pillars very cost efficient.

Earlier research has been done on the thermal effects of salt pillars. Majorowicz and Minea [9], Daniilidis and Herber [3], Manhenke and Beer [10], Petersen and Lerche [14], Li et al. [8] and Yu et al. [21] all find that in their models, that are based on temperature observations close by the salt structures (Fig. 1), the subsurface temperature around the top of the salt pillar is higher than the normal temperature at that depth and that the temperature at the bottom and under the salt pillar or other salt structures is lower than the normal temperature at that depth. Petersen and Lerche [14],

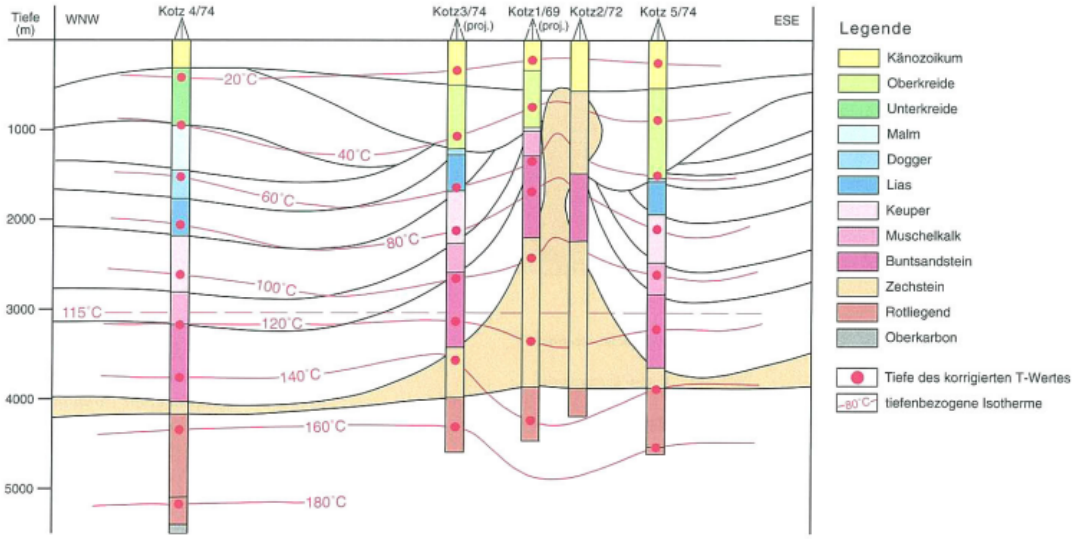

Figure 1: Cross section showing temperature isotherms based on well data around the Kotzen salt pillar in Germany by Manhenke and Beer [10]

In the Netherlands salt pillars exist mostly in the northeast, in and around the Groningen province (Van Gent et al. [20]). These salt pillars consist of salt from the Zechstein unit which through halokinesis formed pillars, walls and pillows. Some of these salt structures are used for the mining of sodium and magnesium salts but none of them have been considered for geothermal energy. Salt caverns are also used for the storage of gas (Hoelen et al. [6]). Research has been done by Daniilidis and Herber [3] on the geothermal potential of salt structures at depths of around 2 - 3km. Shallower salt pillars exist which could be considered for geothermal energy as well.

In the vicinity of Onstwedde, a quaint village in the east of Groningen, a salt pillar rises from a depth of roughly 4000m to only 500m below the surface (Fig. 3). In 2022, an exploratory drilling operation was conducted near this salt pillar, aiming to harness thermal energy (Henk Kombrink [5]). This drilling reached a depth of approximately 300 meters. Surprisingly, the temperature recorded at the bottom of the bore hole fell significantly below initial expectations of elevated temperatures (The expected temperature was 25 °C, and the temperature that was found was 16 °C). This temperature was even lower than what one would anticipate based on standard geothermal gradient of 31.3 °C/km (Bonté et al. [1]). This unexpected result raises intriguing questions, not only about the accuracy of the drilling endeavor but also regarding the impact of salt pillars on local temperature gradients.

The primary objective of this project is to investigate whether the temperature at the summit of the salt pillar shows higher values and to assess the potential for improved results through additional drilling activities, provided they are executed with precision. The approach involves refining existing seismic interpretations in the region. Subsequently, these refined interpretations, in conjunction with the thermal properties of the geological layers and consideration of boundary conditions, will be utilized to construct a comprehensive 3D temperature model around the Onstwedde salt pillar.

Figure 2: Locations of wells near Onstwedde

Table 1: Geological Formations and Compositions from Nlog TNO-GDN [18]

Formation Abbreviation	Formation Name	Composition
NU	Upper North Sea Group	Clay (fine or coarse sand)
NLNM	Lower North Sea Group (and Middle North Sea Group)	Clay and sand
CK	Chalk Group	Carbonate rocks
KN	Rijnland Group	Clayey marls (may contain sandstone at the bottom)
S	Upper Jura Supergroup	Mainly clay
AT	Altena Group	Mainly fine clay
RN	Upper Germanic Trias Group	Silty clay, evaporites, carbonates, and sandstones
RB	Lower Germanic Trias Group	Red sandstones, siltstones, and claystones
ZE	Zechstein Group	Evaporites and carbonates
RO	Upper Rothliegend Group	Conglomerates, claystones, evaporites, and red sandstones

Geology of the Groningen subsurface In Table 1 and fig. 3, a summary is shown of the geological formations and their compositions around the Onstwedde salt pillar. The Zechstein group (at this location mostly consisting of Salt) is mainly overlain by marine sediments with differentiating properties. Overall the overlying layers consists of materials with a much lower thermal conductivity than the Zechstein salt, which can be seen in the cross section through Onstwedde is shown in Fig. 3. A thickness map of the Zechstein layer can be seen in Fig. 4. This map shows the presence of salt pillars in the NE Netherlands.

During the Elsterien ice age, Peelo (Nederland [11]) glacial incisions cut through parts of the upper north sea group. Exactly above the Onstwedde salt pillar such a channel can be found (Fig. 3). The stratigraphy in these channels is characterized by coarse sediments at the bottom and fine clay at the top (Kluiving et al. [7]). The channel above the Onstwedde salt pillar in the cross section is about 160m deep. only the bottom 20 metres or so consist of coarser material and the rest mainly consists of fine clay (based on well data from B07H0080 (Nieuwolda), Nederland [11]). The fine clays formed because after the ice age the channels filled with still water, which caused really low and fine grained sedimentation.

The temperature gradient in The Netherlands is 31.3 °C/km with an average annual surface temperature of 10.1 °C (Bonté et al. [1])

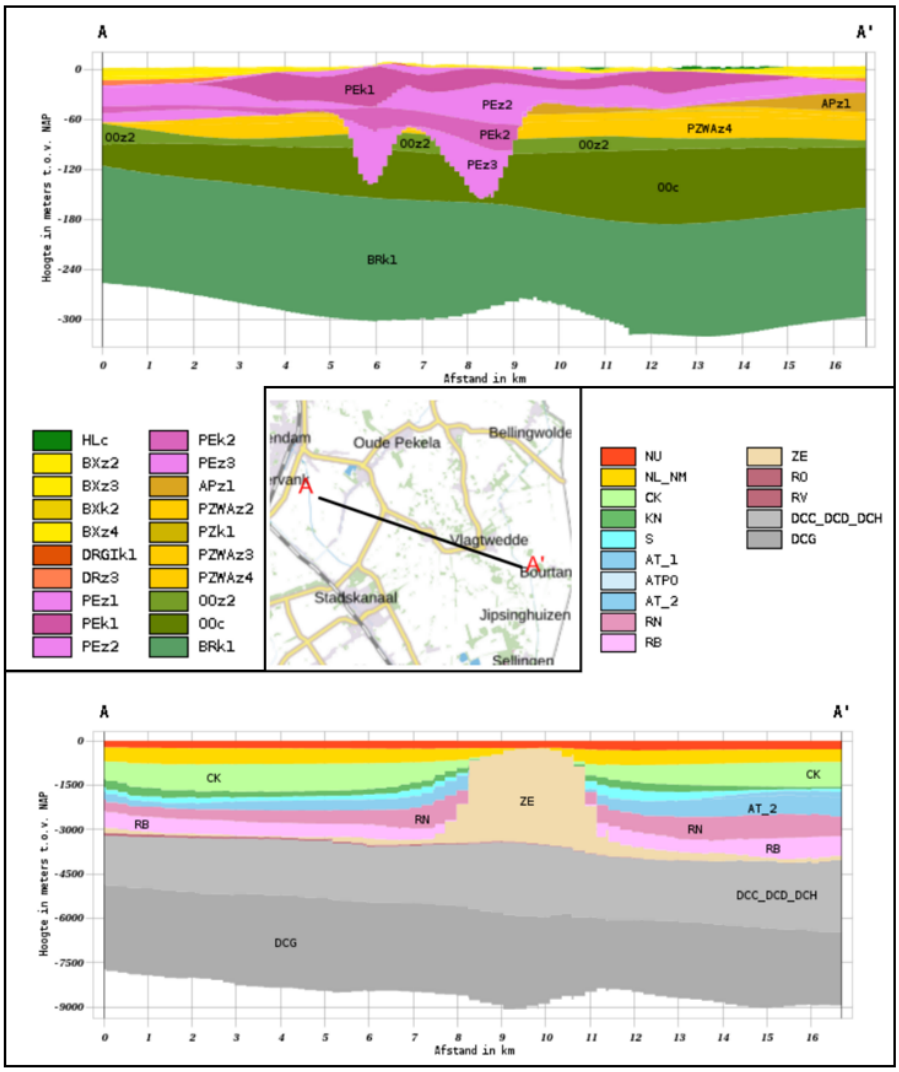

Figure 3: Cross section through Onstwedde, top shows the shallow depths (down to 300 metres) and the bottom shows a deeper cross section (down to 9000 metres). Cross sections are made on DINOLoket [18], with BRO REGIS II v2.2.1 (top) and DGMDiep v5.0 (bottom)

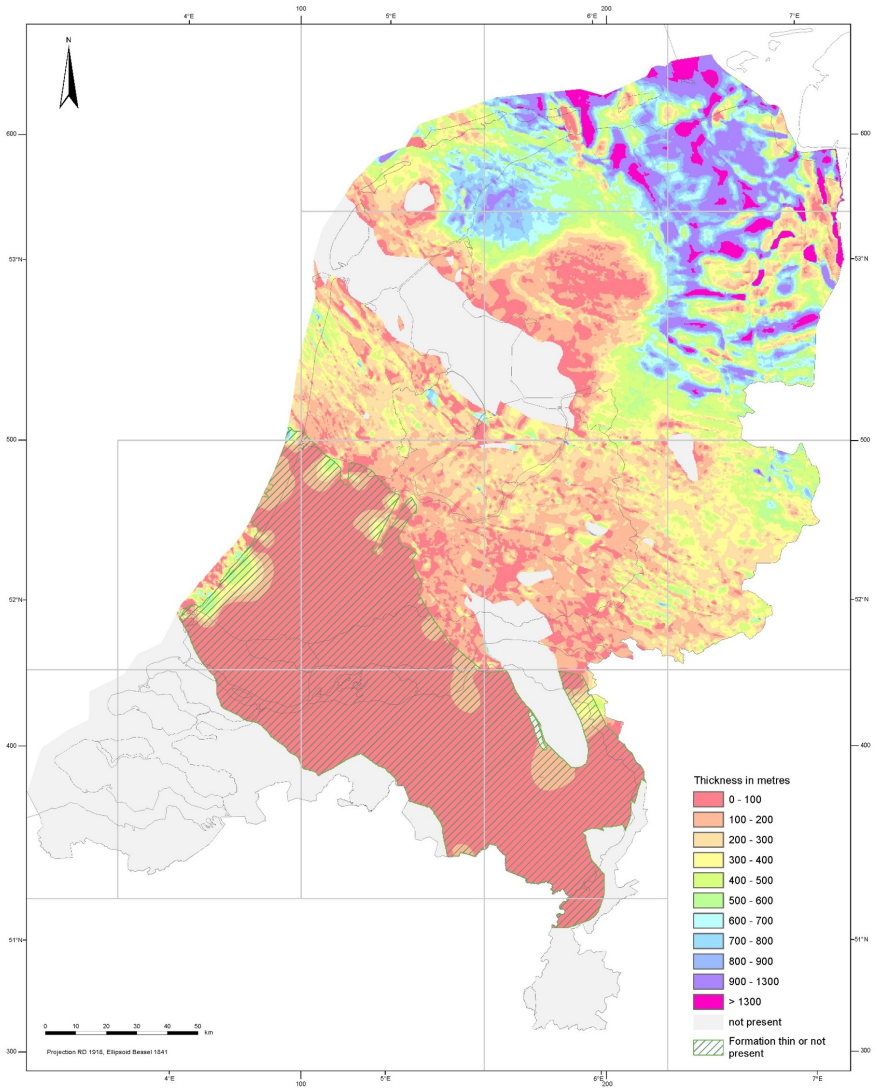

Figure 4: Thickness map of the Zechstein layer from DGMDiepV-4(NLOG - Netherlands Petroleum Data Management [12])

3 Construction of a static model of the Onstwedde salt pillar

3.1 Method: re-interpretation of seismic and well data

Seismic interpretations of the region are currently accessible within DGM-Diep; however, these interpretations are conducted on a broad scale and lack the necessary detail, particularly in the vicinity of the salt pillar, to construct a precise temperature model. To address this limitation, more intricate interpretations are generated using Petrel, a subsurface modeling program. The seismic data is initially presented in two-way travel time, necessitating the conversion of interpretations into depth. The modeling process in Petrel can be divided into three main phases (Fig. 5). First is the Preparation which consists of the import of the data and defining the key horizons. For the input of the data multiple seismic cubes in two way travel time are available and compared to find which has the best and most accurate resolution of the area. Wells are imported that are located in or near the seismic cube. These wells are used to calibrate the interpretation at the points of the wells. DGM Diep 4 is used as benchmark for the seismic interpretations in the area. DGM Diep is a model of the main geology of the Netherlands and consists of interpretations of the 13 best defined layers in the subsurface of the Netherlands (TNO-GDN [18]). DGM Diep 5 is also available but there are no significant diferences in interpretations in the study area so DGM Diep 4 is used for the sake of consistency as DGM Diep 5 was not yet available at the start of the project. An unpublished TNO dataset for the interpretation of the Peelo group is used.

Defining the key horizons is done by looking at the strong reflectors in the seismic cubes. Most of the important layers are already connected to key horizons in DGM Diep. In the seismic cube between the DGM Diep interpretations of the RB and AT unit a difference can be seen between the top part (strong reflectors) and the lower part (weak reflectors). Well correlation shows that this is the top of the RN, which is subsequently interpreted as well. Lithostratigraphic data from multiple wells in the region is available, and used to refine interpretations in those specific zones and establish correlations between the seismic lines and lithostratigraphic units. While there are faults within the study area, they exhibit minimal offset, and as such, they are not used in the interpretation.

The second stage of the workflow involves initially selecting the horizons required for interpretation. Subsequently, for each interpreted unit, a surface can be generated, extending across the entire extent of the seismic cube. Since not all surfaces are consistently present across the entirety of the cube, relationships between surfaces are established where layers terminate on other layers. The majority of layers end on the salt pillar; however, for the purpose of time-depth conversion, it is essential for all layers to span the entire cube. To address this, layers terminating in the salt pillar are interconnected to trace the top of the salt at the summit of the pillar. Consequently, above the salt pillar, every layer is technically present, albeit with a thickness of 0.

The third step is the depth conversion. VELMOD-4 (velocity model from NLOG NLOG - Netherlands Petroleum Data Management [13]) is a model to convert stratigraphic units in the subsurface of The Netherlands from TWT (two way travel time) to depth. The formula used for each layer is v0 + k*z. k is a constant determined in VELMOD, V0 is a velocity field that is created for the whole of The Netherlands in VELMOD. The salt of the Zechtstein follows a different formula (the velocity in rock salt does not scale with depth). The Vint velocity field for the ZE is made for the whole of The Netherlands but skips complex structures like salt pillars. To get an accurate time to depth conversion directly underneath the salt pillar the depth of the base of the salt is interpolated between the converted depths at the sides of the salt pillar. Once all of the surfaces have been converted to depth they can be exported to use for the thermal modeling.

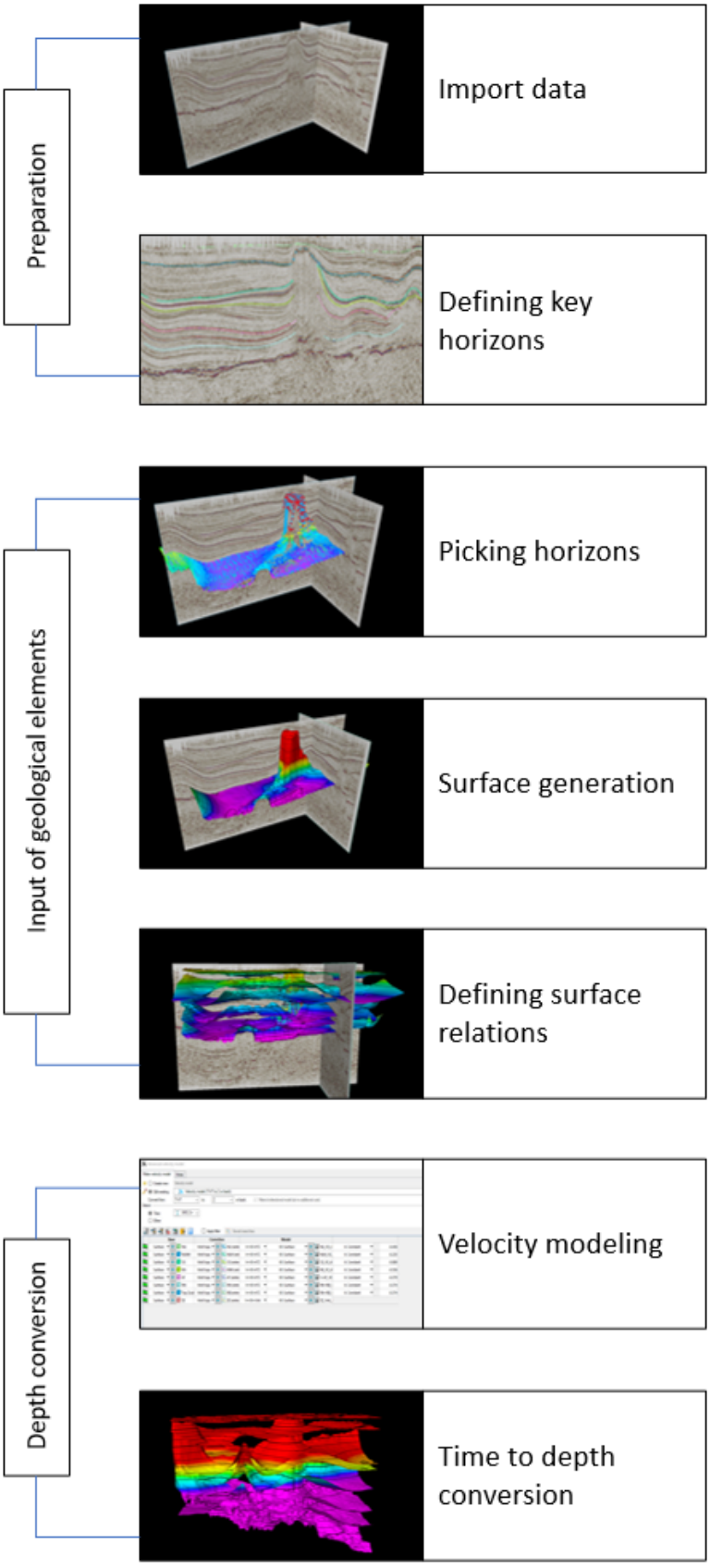

Figure 5: Workflow in Petrel

3.2 Results: new 3D static model

In fig. 6 the interpretation of the layers in depth is presented. The salt pillar is clearly visible in the center and at the edged of the study area parts of other salt pillars / salt structures can be seen. Fig. 7 shows the interpretation of the Peelo layer, which is situated exactly on top of the salt pillar. These models with the interpretations are used for the thermal modeling.

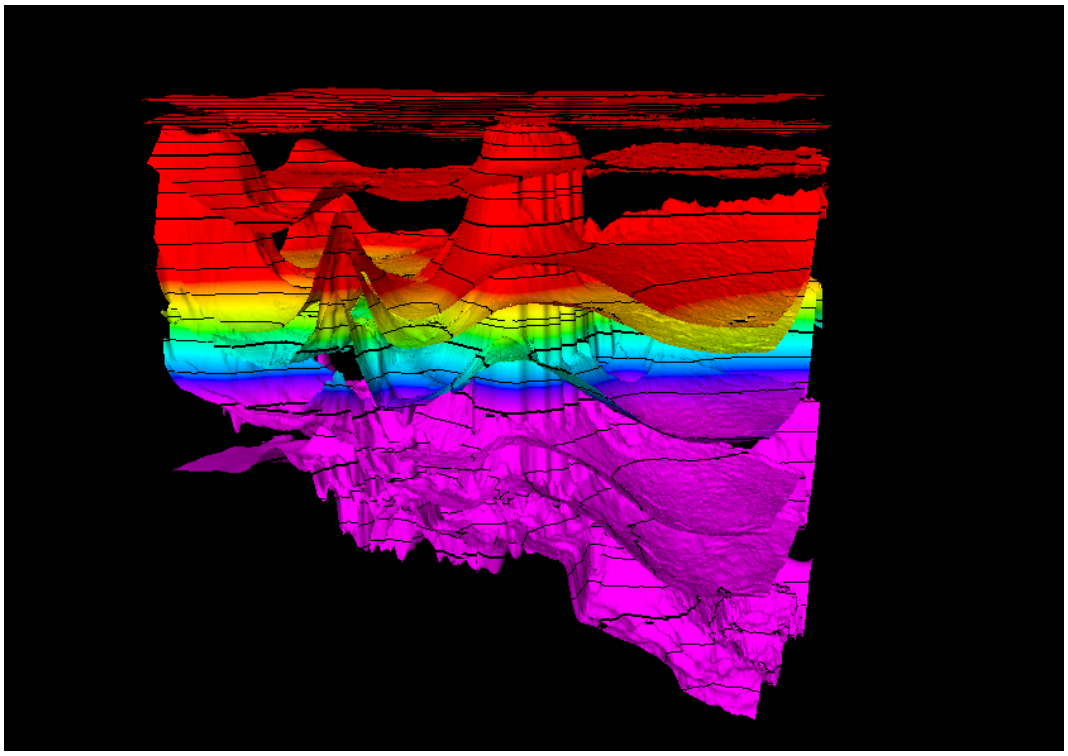

Figure 6: New 3D static model of the Onstwedde salt pillar, constructed from a detailed reinterpretation of all available seismic and well data

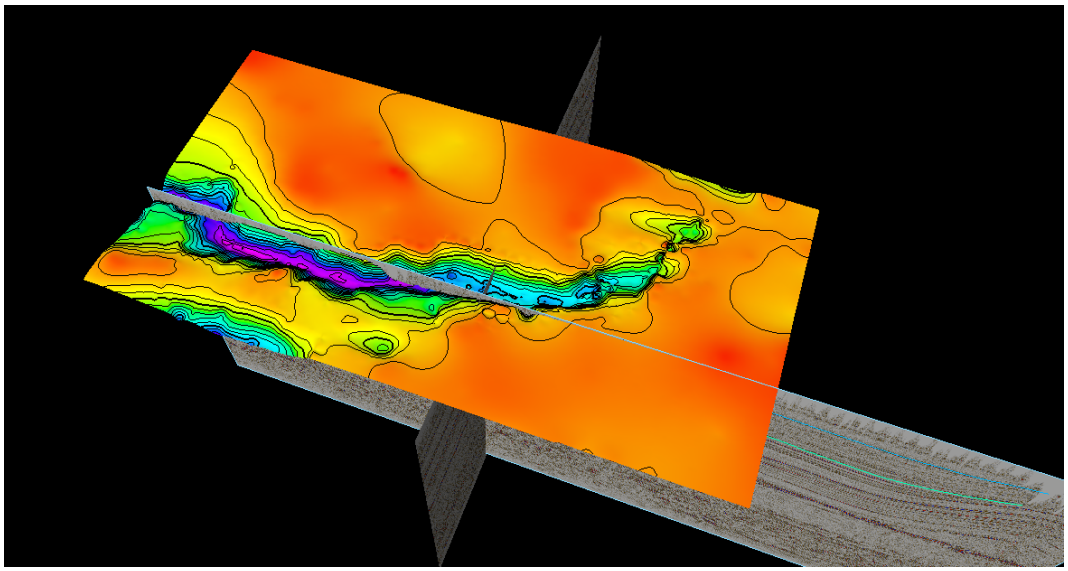

Figure 7: Interpretation of the base of the Peelo layer

4 Temperature model of the Onstwedde salt pillar

4.1 Method: numerical thermal modelling

4.1.1 Modelling approach and software

Basin3D, an in-house program developed by TNO Bonté et al. [1], is employed for modeling temperature and heat flow in the subsurface. The program takes inputs from interpreted layers in Petrel, incorporating properties such as thermal conductivity for each layer, along with specified boundary conditions for the model's top and bottom (8). A surface temperature of the (approximate) average of 10 °C is taken for the top boundary (Bonté et al. [1]), while the complexity of the bottom boundary condition will be elaborated upon in subsequent chapters. The model solves a transient 3D temperature equation:

$$\frac{\partial T}{\partial t} = \frac{1}{\rho C_p}\left[\nabla\cdot(k\nabla T)+A\right] - v_z\frac{dT}{dz} \quad \text{with}\ \nabla = \left(\frac{\partial}{\partial x},\frac{\partial}{\partial y},\frac{\partial}{\partial z}\right)^T \quad \text{(Eq. 1)}$$

Where T = teperature, ρ = density, Cp = specific heat, k = thermal conductivity, A = radiogenic heat production and vz is vertical velocity.

The temperature modeling process is split into two steps (Fig. 8). The initial step involves modeling temperature in a multi 1D fashion, wherein the temperature gradient from the bottom to the top is calculated for each point. Subsequently, the second step transitions the multi 1D model into a 3D model, introducing lateral heat flow into the analysis.

Several temperature models are generated, including a straightforward comparison between the 1D thermal gradient in a salt pillar and the thermal gradient within a conventional stratigraphic sequence. This model aims to illustrate the contrast between the standard scenario and the conditions within a salt pillar, characterized by a notably higher thermal conductivity. Other models focus on the study area and create a 3D temperature model around the salt pillar. Within these models the boundary conditions and other inputs are varied to study the effects and significance of those inputs. The varieties in inputs consist of altering the thermal conductivities of the salt and the overlying layers, the lower boundary condictions and the presence of a glacial incision on top of the salt pillar.

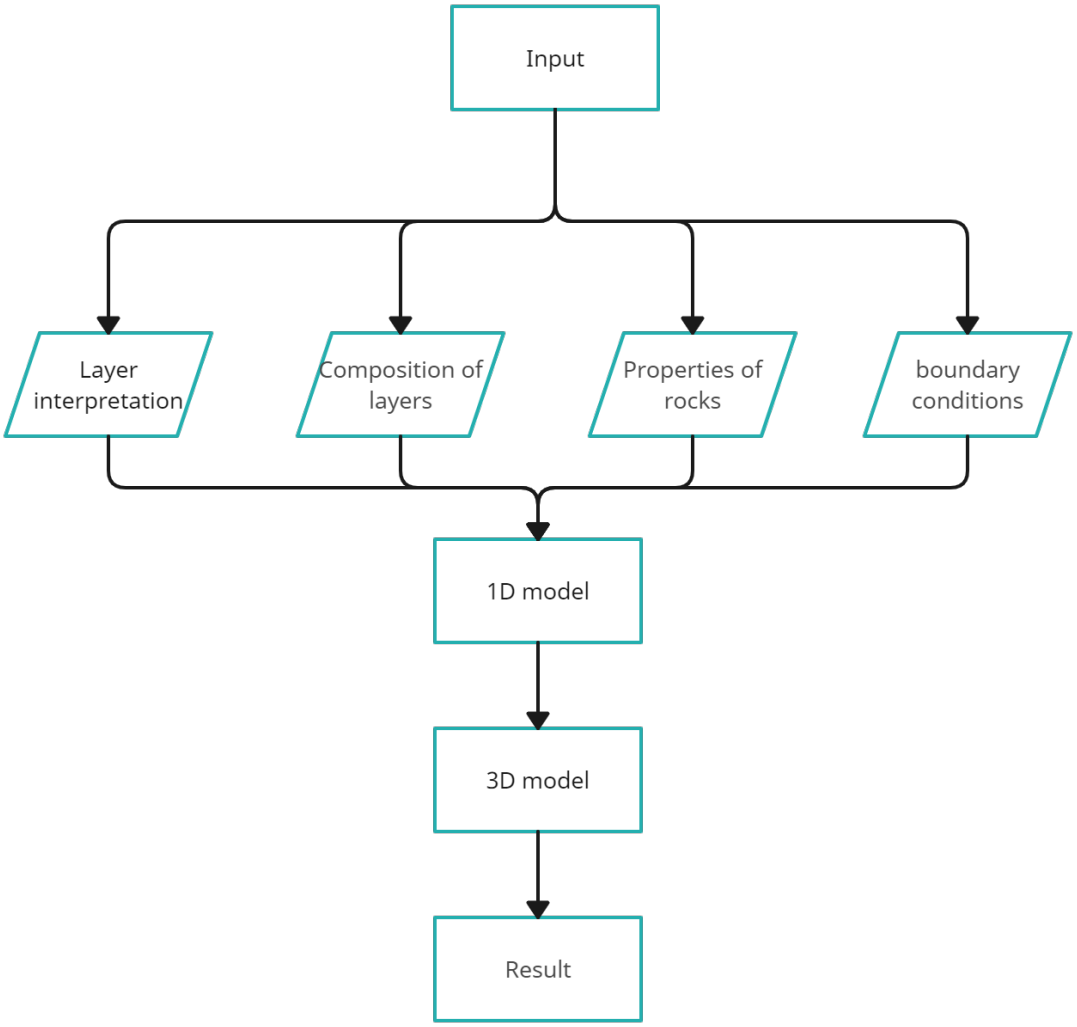

Figure 8: Workflow in Basin3D

4.1.2 Material properties

The composition of each layer is based on data from Nlog. Lithological compositions are based on the lithological conmpositions of the same layers in wells close to Onstwedde. The geological composition of each group can be seen in Table 2.

Distinct rock types exhibit varying thermal conductivities. Consequently, for each lithological unit, a weighted average thermal conductivity is calculated by combining the thermal conductivities and other characteristics of individual rock types present within the unit. The thermal conductivity data is sourced from Hantschel and Kauerauf [4] (Table 3. The methodology also accounts for the impact of depth-related factors such as porosity, pressure, and temperature on thermal conductivity. Fig. 9 shows the relation between the porosity of the rocks and the thermal conductivity at depth. Notably, the data lacks a scaled thermal conductivity value for salt, which is described by Urquhart and Bauer [19]. different models are made for a parameter study where both the multi 1D and the 3D model have to run again. The 3D modeling also has the option to calibrate the model with nearby temperature data from wells but as there are no wells with temperature data close by, this option is not used. A cross section of the different values for the thermal conductivity can be seen in Fig.10. The differences in thermal conductivities also roughly show the stratigraphic units. The large thermal conductivity of the salt is clearly visible in the cross section.

4.1.3 Determining boundary conditions

Concerning the boundary conditions, the temperature at the top of the model, corresponding to the surface, is set at 10 °C. Determining the temperature at the bottom of the model poses more challenges. Burkitov et al. [2] has produced a temperature map at the bottom of the Rothliegend, indicating a temperature of 120 °C at a depth of 3960m. However, it's important to note that this temperature map, derived from well data, doesn't precisely account for smaller structures like salt pillars, and their potential influence on temperature is not accurately represented.

Given that the bottom of the Rothliegend is not significantly lower than the salt pillar, and considering the potential impact of the salt pillar on temperature, a more nuanced lower boundary condition may be necessary for achieving more precise and accurate modeling results.

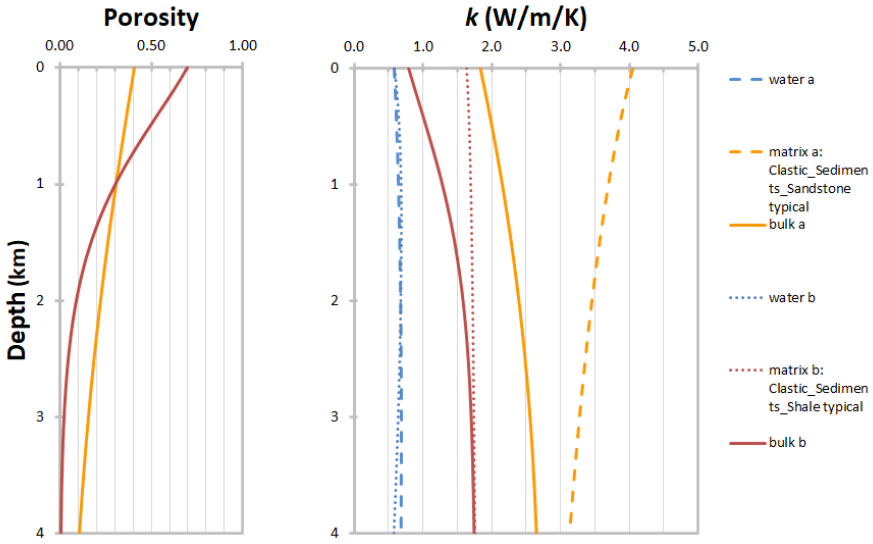

Figure 9: Effect of the porosity in rocks on the thermal conductivity at depth basen on data from Hantschel and Kauerauf [4]

Table 2: Geological compositions of each unit (percentage)

Abbreviation	Sand	Shale	Chalk	Marl	Salt	Micrite
PE	0	100	0	0	0	0
NU	50	50	0	0	0	0
NMNL	25	75	0	0	0	0
CK	0	0	100	0	0	0
KN	0	10	0	90	0	0
AT	50	50	0	0	0	0
RN	0	40	0	0	40	20
RB	0	100	0	0	0	0
ZE	0	0	0	0	100	0
RO	100	0	0	0	0	0

Table 3: Material Properties of the different rock types present in the lithologies, taken from Hantschel and Kauerauf [4]

ID	**K [W/mK]**	**Anisotropy**	**cp [J/kgK]**	**Sorting**	**rho [kg/m3]**	**A [W/m3]**	**phi0 [%]**	**k (comp. par.) [1/km]**
Sand	3.95	1.15	855	1	2720	0.7	0.41	0.31
Shale	1.64	1.6	860	1.38	2700	2.03	0.7	0.83
Micrite	3	1.19	835	1.11	2740	0.35	0.51	0.52
Salt	6.5	1.01	860	1	2740	0.02	0	0
Chalk	2.9	1.07	850	1	2680	0.6	0.7	0.9

4.2 Temperature Modelling

4.2.1 1D models - Salt pillar vs normal stratigraphy

The first graph depicts the subsurface stratigraphy within a few hundred meters of the salt pillar, while the second graph illustrates the stratigraphy directly above the salt pillar. In the latter graph, it is evident that most of the layers on top of the salt pillar are absent, with only the NU and the NMNL remaining, albeit in thinner formations due to the salt pillar's formation. Both models extend to a depth of 3743m, reaching the top of the Rothliegend.

Observations from the 1D model reveal that the salt pillar induces increased upward heat flow, resulting in a steep temperature gradient of up to 90 °C between the surface and the salt pillar. The most significant temperature difference between the normal and salt pillar scenarios occurs at approximately 300 meters depth, where the subsurface temperature of the salt pillar is more than 10 °C higher than that of the normal situation. This would suggest that the 3D modelling of the temperature around the salt pillar should result in a positive anomaly at the top of the salt pillar.

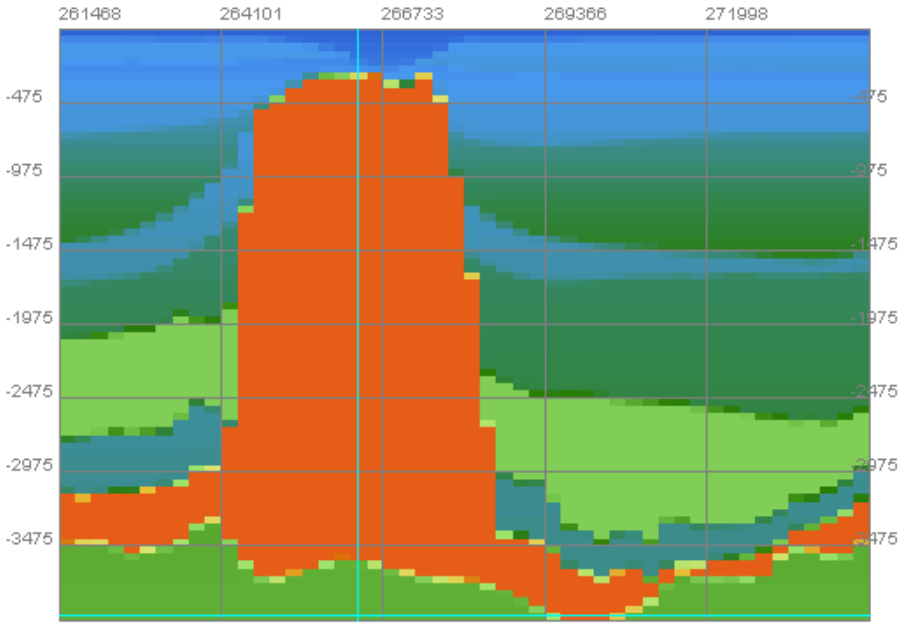

Figure 10: Cross section showing the thermal conductivities (k) of each interpreted layer in Basin3D. colors indicate different conductivities, see Table 3 for values.

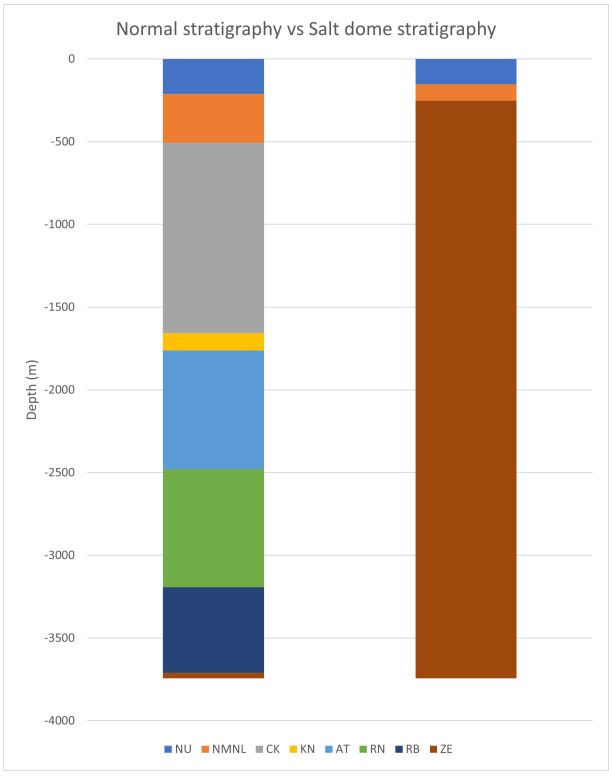

(a) Normal stratigraphy versus the stratigraphy through the salt pillar.

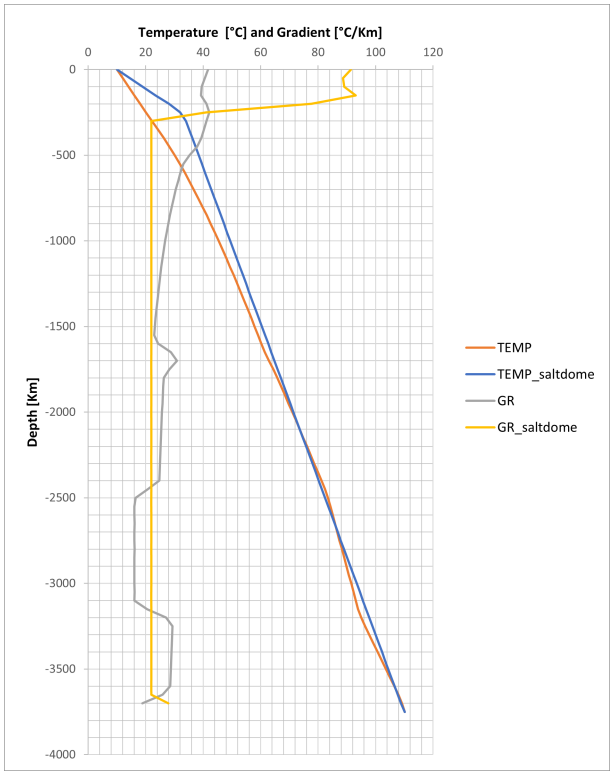

(b) Graphs of the temperature and temperature gradient of both stratigraphies plotted against depth. TEMP: temperature, GR: geothermal gradient.

Figure 11: Comparison of stratigraphies and temperature profiles.

4.2.2 3D models

For each of the 3D models, a multi-1D model is initially generated. The left side of Fig. 12 illustrates the outcome of the multi-1D modeling, revealing a predominantly higher temperature toward the top, particularly to the sides of the salt pillar, thsi is due to the salt not reaching as high at the sides of the pillar and therefore it is less effected by the cool surface, making the spikes in temperature higher. Subsequently, the right side of Fig. 12 demonstrates the results of the 3D modeling, where lateral heat flow is incorporated.

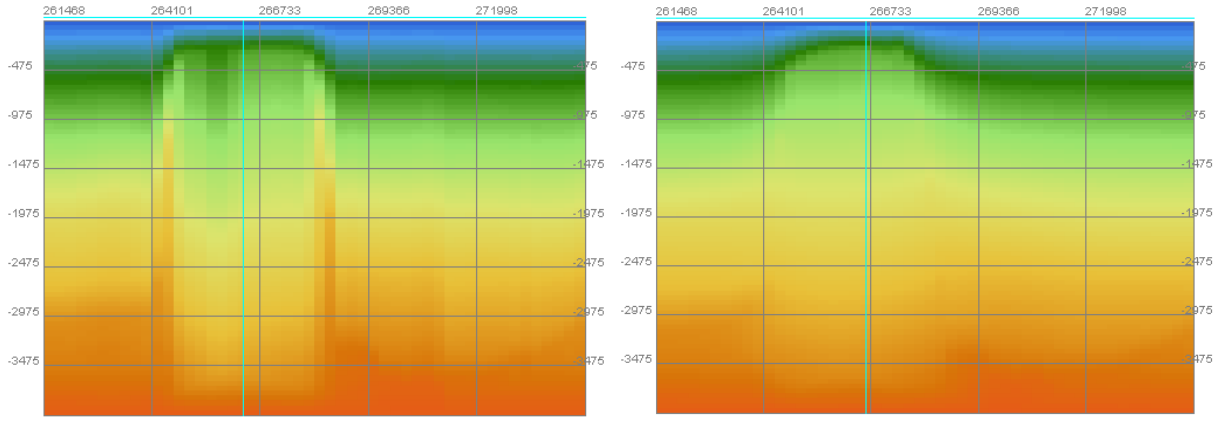

Figure 12: Left: cross section of the temperature in the multi-1D model. Right: same cross section but with the temperature modelled in 3D

Normal model

The primary outcome of this research is the normal model, where the lower boundary condition is set at 120 °C at a depth of 3960m, sourced from the Groningen field review Burkitov et al. [2]. The thermal conductivity of salt is specified as 6.5 W/m K. The left section of Fig. 13 illustrates temperature isotherms in a 2D profile from west to east through the salt pillar. Notably, the temperature isotherms at the top of the salt pillar exhibit a laterally larger temperature where the salt pillar is present. Conversely, at the bottom of the salt pillar, the temperature isotherms display a negative anomaly compared to the surrounding lateral temperatures.

The right graph in Fig. 13 depicts the lateral anomalies of these temperatures. At the top of the salt pillar, a positive lateral anomaly of more than 18 °C is observed, whereas at the bottom of the salt pillar, there is a negative anomaly of more than -3 °C. This outcome indicates that the top of the salt pillar is significantly more affected by temperature differences than the bottom of the salt pillar. This could also be caused by the lower boundary condition which is close to the bottom of the salt pillar. Fig. 14 illustrates the heat flow within and surrounding the salt pillar. The heat flow within the salt pillar is considerably greater than the heat flow around the salt pillar.

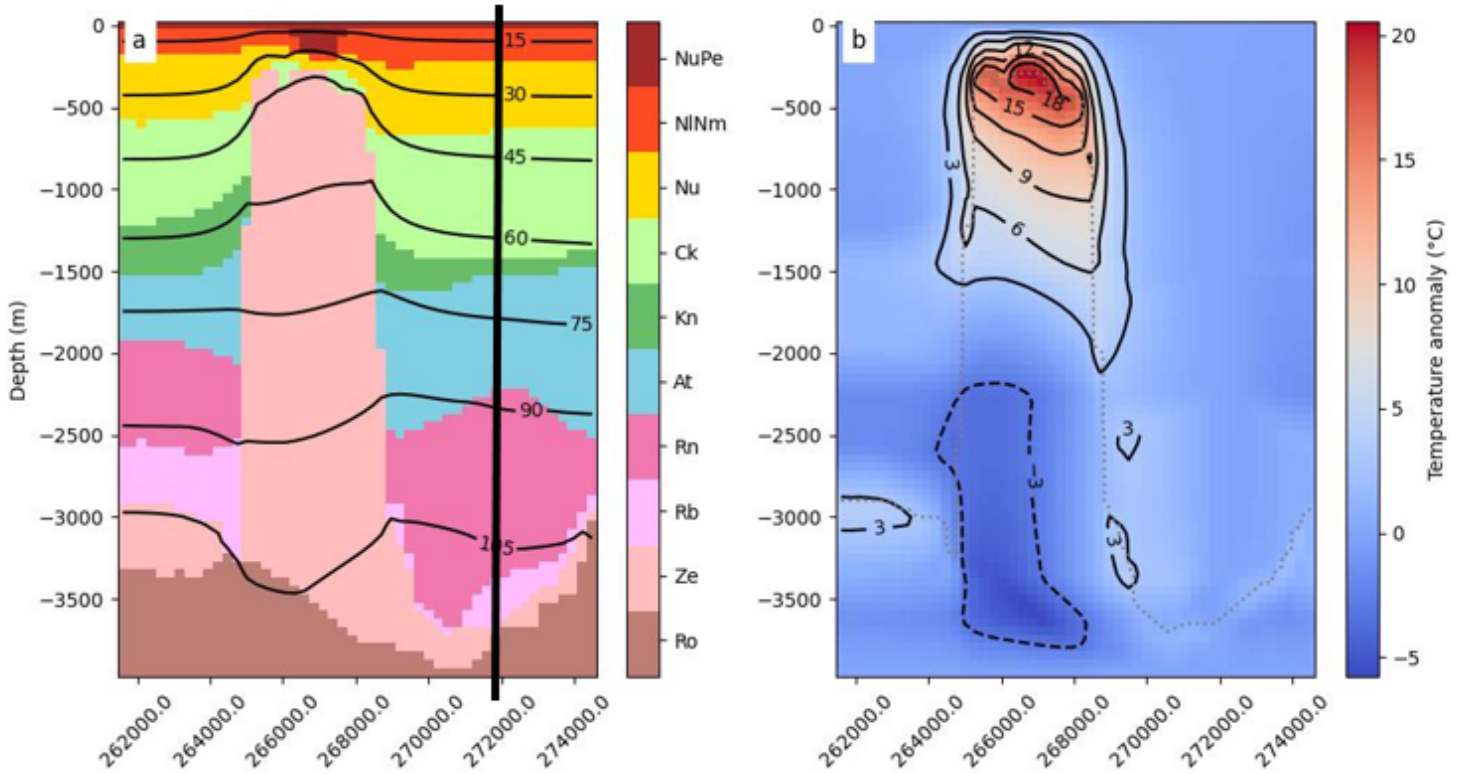

Figure 13: a) Cross section of the stratigraphy and temperature isotherms of the normal model. b) Lateral difference in temperature compared to normal stratigraphy (at the location of the black line in a). The outline of the salt pillar is indicated by the dotted gray line

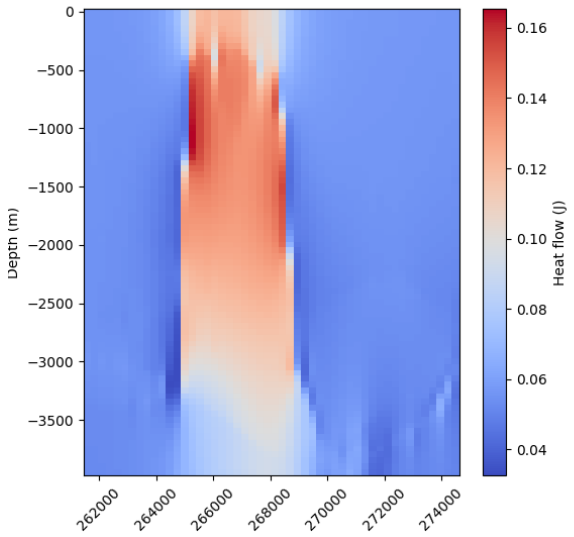

Figure 14: Heat flow in and around the salt pillar

Model with temperature-dependent thermal conductivity of salt

Urquhart and Bauer [19] and Raymond et al. [15] find that the conductivity of salt is depended on the temperature with a decreasing thermal conductivity at higher temperatures. The thermal conductivity of single-crystal halite decreases from 9.975 W/m K at -75 °C to 2.699 W/m K at 300 °C (Urquhart and Bauer [19], Fig. 15). This would suggest that the thermal conducitivy at the bottom of the salt pillar is less than the thermal conductivity at the top which would have a big effect on the resulting temperature profile. With a thermal conductivity of salt dependent on the temperature the vertical temperature gradient would increase in the salt and the temperature anomalies at the top and the bottom of the structure become less (Petersen and Lerche [14]). The scaling salt model has a thermal conductivity of salt that decreases with a factor 0.9 per km, starting with 6.5 at the surface. this is to roughly replicate the scaling thermal conductivity of salt with temperature from Raymond et al. [15]. The results show a slight temperature difference between the top and the bottom of the salt pillar compared to the normal model (16). Fig. 17 shows the difference in temperatures between the normal model and the scaling salt model on the same cross section. At the summit of the salt pillar, the temperature is approximately 3 °C lower than in the normal model. Nonetheless, this still yields an anomaly of up to +16 °C compared to the temperature away from the pillar at the same depth.

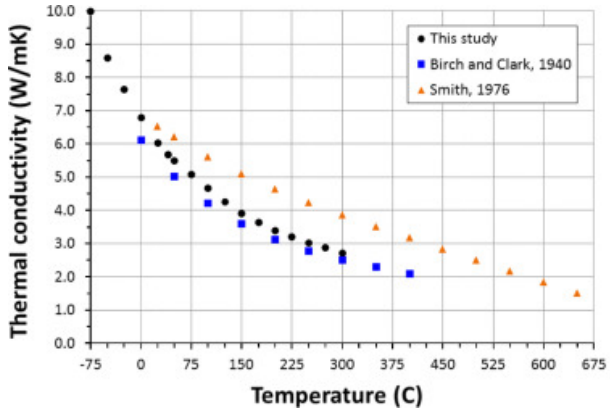

Figure 15: Thermal conductivity of salt versus temperature from Urquhart and Bauer [19]

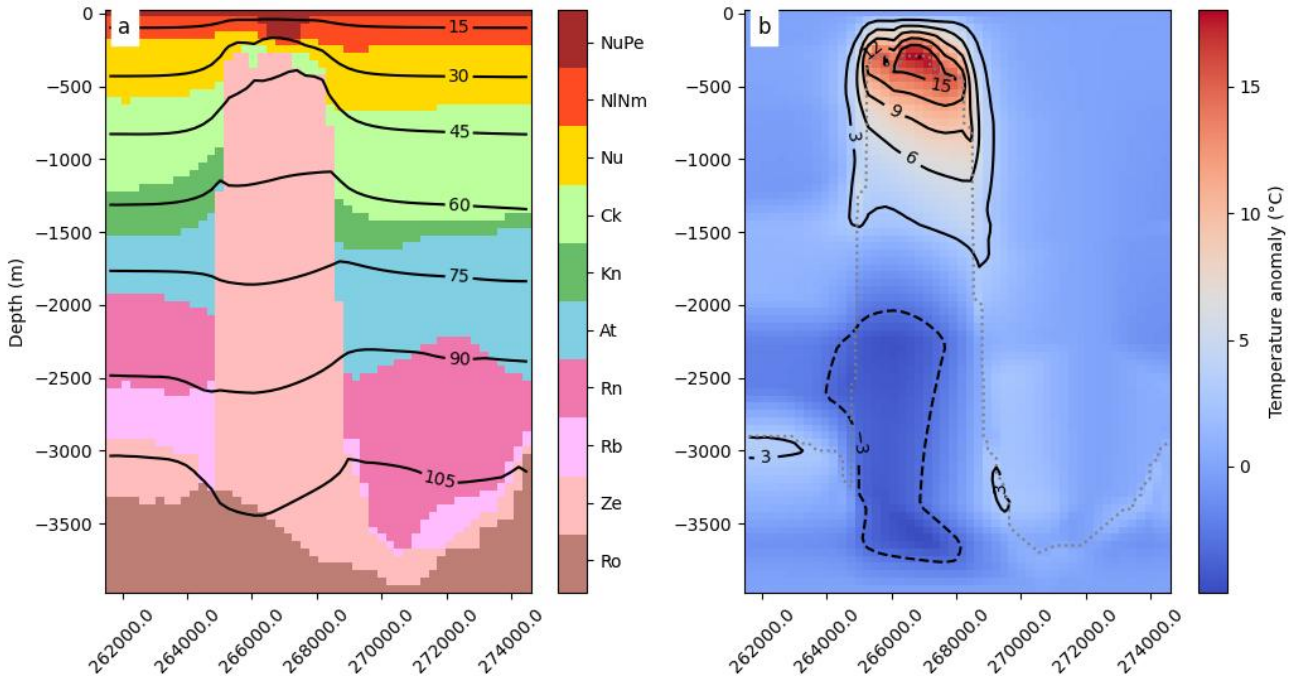

Figure 16: Model with a scaling thermal conductivity of salt

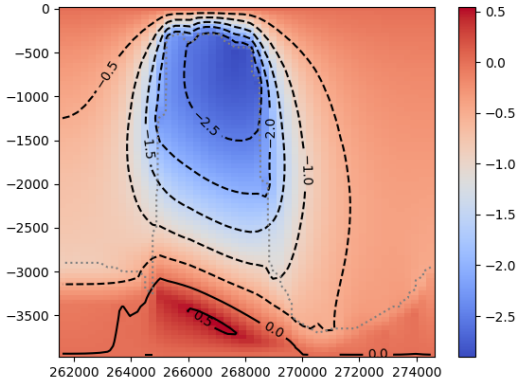

Figure 17: Difference in temperature between the scaling salt model and the normal model

Model without glacier channel

In this case study, it is coincidental that the Peelo glacier channel is located precisely on top of the salt pillar. This channel primarily contains fine-grained mud, resulting in a layer with low thermal conductivity. To enhance the model's comparability to other salt structures in the area, the channel is omitted from the model. The outline of the channel remains visible in the model, but in terms of thermal properties, it is treated the same as the NU layer (Fig. 18). The difference between this modified model and the normal model is a minor temperature decrease at the top of the salt pillar, approximately 3 °C (Fig. 19). Otherwise, no significant differences are apparent. This observation suggests that, in this particular case, the Peelo channel might function as a kind of insulating thermal lid, impeding the upward movement of heat at the top of the salt pillar.

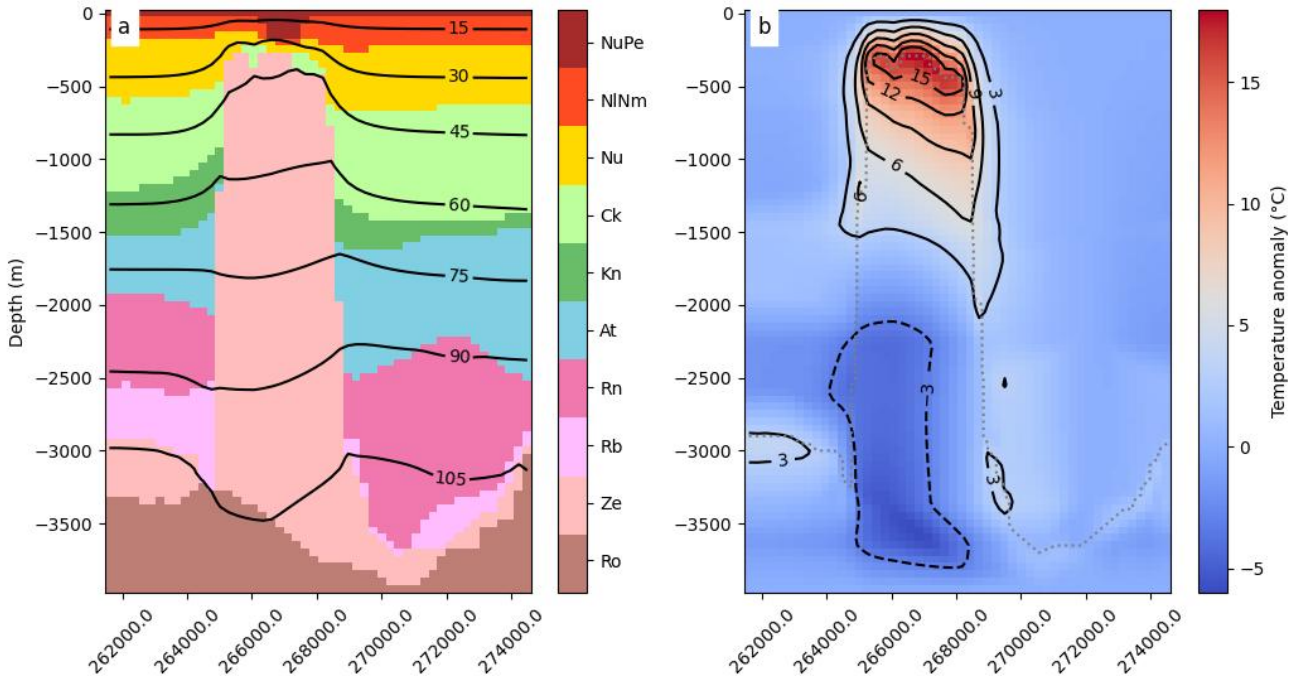

Figure 18: Model without the Peelo channel on top of the salt pillar

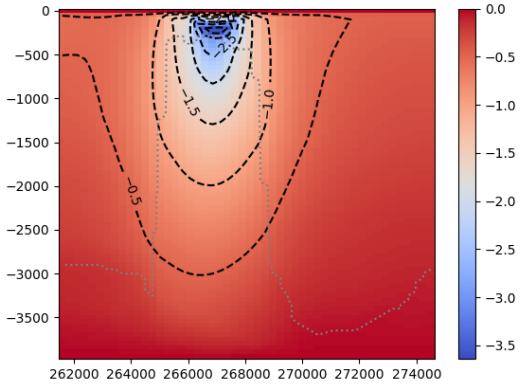

Figure 19: Difference in temperature between the no Peelo model and the normal model

Model with a lowered bottom boundary condition

The accuracy of the lower temperature boundary condition is compromised, given the absence of detailed temperature measurements at depths exceeding 3000m in the region. Considering that the salt pillar extends to a depth of around 3500m, the thermal impact of the salt pillar could influence temperatures beyond the initially set boundary condition of 3960 meters. To assess this impact, an alternative lower boundary condition is introduced.

This model incorporates a lower bottom boundary condition of a fixed 150 °C at a depth of 5000m (Fig. 20). The results of the model demonstrate similar temperature anomalies at the top of the salt pillar (Fig. 21). However, at the bottom of the salt pillar, the temperature anomalies are significantly higher. The lateral differences at the bottom of the salt pillar now exceed 18 °C lower than the temperature at the same depth away from the pillar. It's important to note that a caveat in the modeling process was the determination of the lower boundary condition (temperature at different depths). However, this model indicates that the uncertainties of the lower thermal boundary condition have a limited effect of only a few degrees Celsius on the predicted temperature anomaly at the top of the salt pillar.

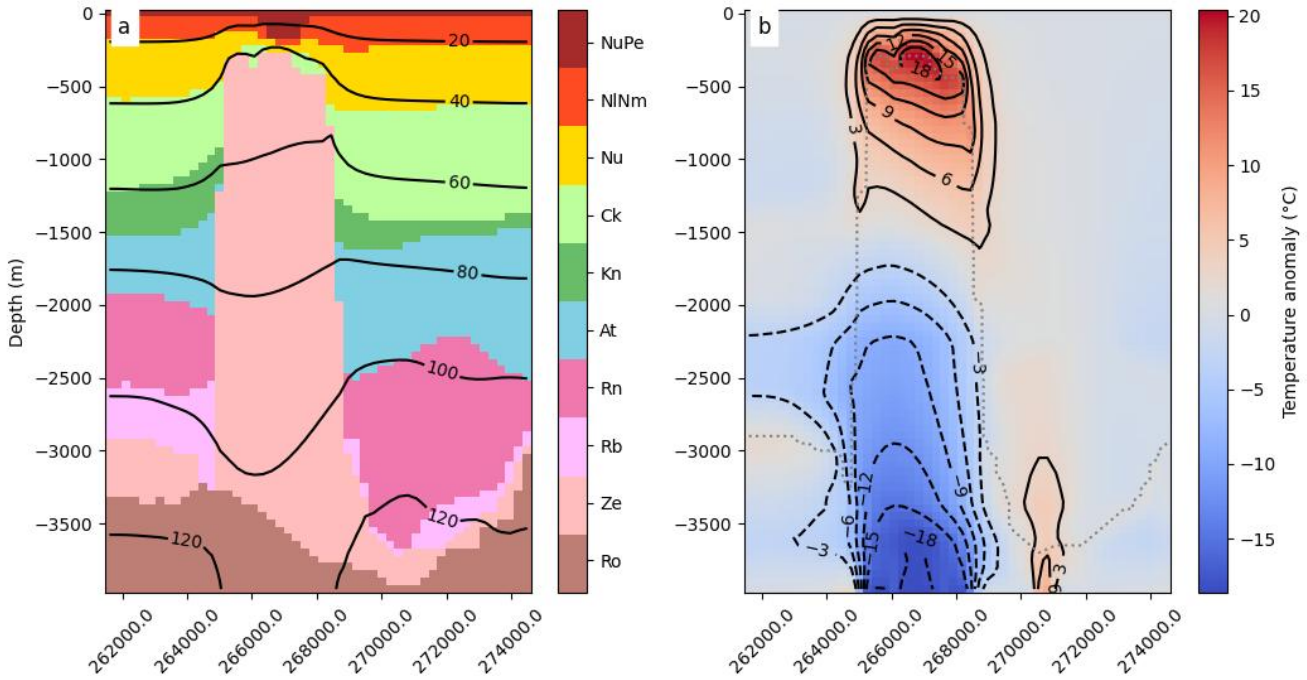

Figure 20: Model with a boundary condition of 150 °C at 5000 metres

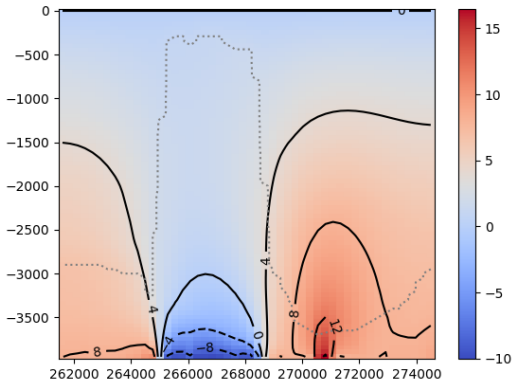

Figure 21: Difference in temperature between the model with a boundary condition of 150 °C at 5000 metres and the normal model

Models with varied thermal conductivities

There are no exact values for thermal conductivities of the different lithostratigraphic groups in the subsurface of Groningen because they often consist of a mix of multiple different materials. Hantschel and Kauerauf [4] present values for thermal conductivities of certain materials (e.g. sandstone, shale). These thermal conductivities are used for each layer to make a weighted average thermal conductivity for the complete layer. This weighted average also takes pressure and porosity in consideration. The composition of each layers is given in data from Nlog. Not every sandstone has exactly the same thermal conductivity and the compostion of each layer can vary laterally. To take this into consideration models are made with relative higher and lower thermal conductivities of the overlying layers (from -30 to +30 percent). Results of the temperature variations between these different conductivity models can be seen in fig. 22. The figures show that with lower thermal conductivities the temperature at the top of the salt pillar becomes higher than in the normal model and less heat from the salt pillar is transferred to the surrounding layers making them a bit cooler. In the models with higher thermal conductivities for the overlying layers the temperature at the top of the salt pillar becomes a bit less compared to the normal model and the layers around the salt pillar become a bit warmer. Almost all of these differences do not become more than +- 2 degrees. So it is reasonable to conclude that even though the thermal conductivities of the layers are not well known, the possible variance in their values insufficient to significantly affect the temperatures in and around the salt pillar.

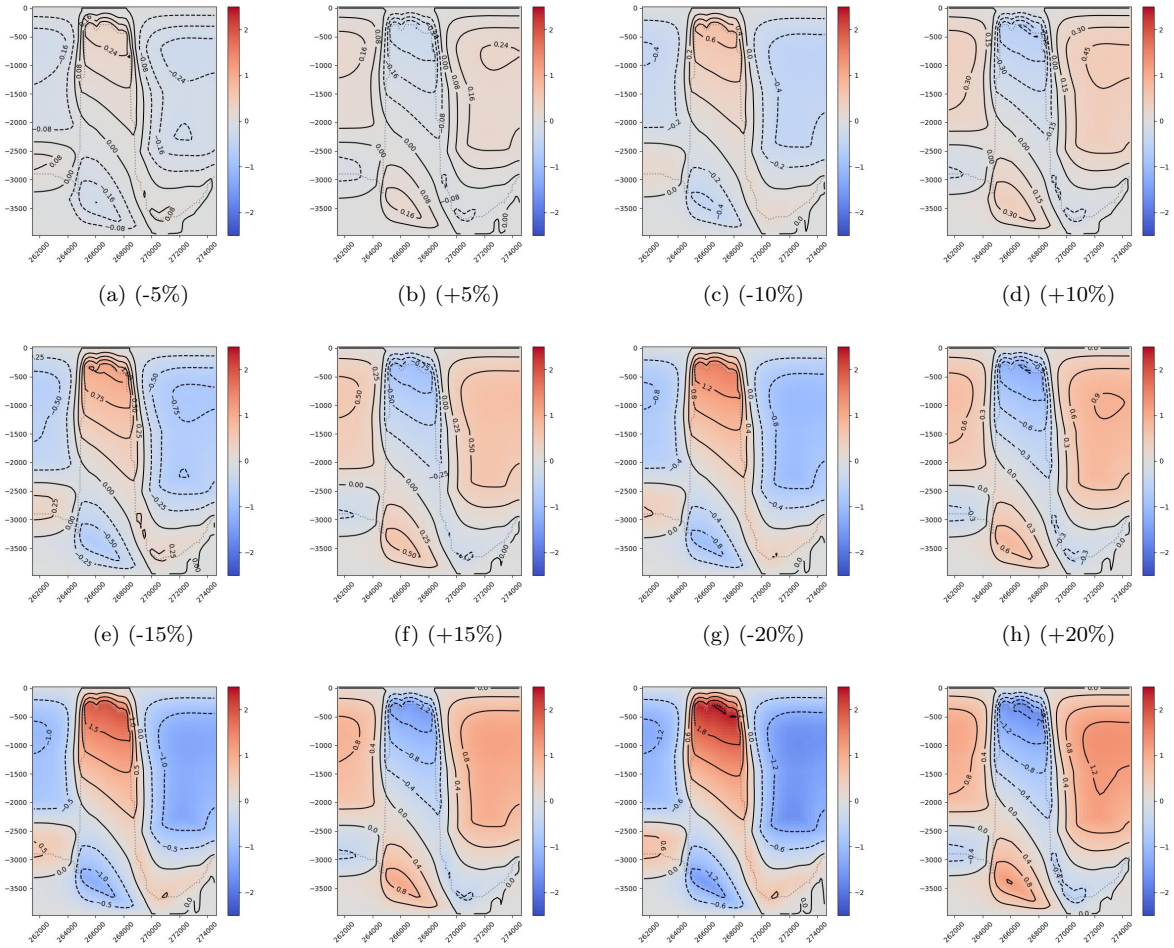

(a) (-5%) (b) (+5%) (c) (-10%) (d) (+10%)

(e) (-15%) (f) (+15%) (g) (-20%) (h) (+20%)

(i) (-25%) (j) (+25%) (k) (-30%) (l) (+30%)

Figure 22: Variations on the thermal conductivities of the layers overlying the Zechstein.

5 Discussion

The overall model reveals a lateral positive temperature anomaly at the top of the salt pillar, with the anomaly being more pronounced in the central region, reaching temperatures up to 20 °C higher than those at the same depth away from the pillar. A parameter study is conducted to explore how specific factors impact these results. The results in temperature profiles coincide with the temperatures from the well data from Manhenke and Beer [10].

5.1 Parameter study

- Introducing a scaling thermal conductivity of salt with temperature leads to a more gradual temperature profile in the salt pillar, resulting in a slightly lower temperature at the top of the pillar.
- The removal of the Peelo glacier channel above the salt pillar highlights its lid-like effect as a thermal insulator. Without the channel, heat retention at the top of the salt pillar is reduced, causing a few degrees lower temperatures compared to the normal model.
- A lower boundary condition primarily affects the bottom of the salt pillar, causing it to become laterally cooler compared to the layers away from the pillar at the same depth. Interestingly, temperatures at the top of the pillar do not seem significantly affected by different lower boundary conditions. Given that the lower boundary condition is the least known factor in the model, the fact that it does not substantially influence the top of the pillar is advantageous, as it reduces the urgency for further research on the lower boundary condition.
- Variations in the thermal conductivity of the overlying layers introduce some fluctuations in temperatures at the top of the salt pillar, but these variations are not substantial and still result in a significant temperature anomaly at the pillar's summit.

5.2 Implications for geothermal energy exploitation

The findings from this research offer compelling insights for thermal energy exploration. The models suggest that when drilling on top of a salt pillar, it may be possible to achieve a certain temperature with drillings that are hundreds of meters less deep compared to drilling in the normal subsurface. Given that drilling constitutes a substantial portion of the overall expenses in such processes, this discovery could significantly reduce the cost of generating thermal energy, especially in regions with abundant salt pillars.

In the Netherlands, particularly in Groningen, numerous salt pillars and other salt structures from the Zechstein formation are present. If drillings in and around a salt pillar can confirm that the temperature at the top of a salt pillar is indeed higher, numerous possibilities emerge for harnessing thermal energy from these salt pillars. Some of these salt pillars are situated beneath cities and villages, presenting an excellent opportunity to utilize the thermal heat for heating homes and other buildings.

It is crucial, however, to conduct drillings at the center of the salt pillar. As evident in the models, the temperature anomaly significantly diminishes at the sides of the salt pillar, emphasizing that drilling at the periphery would not fully capitalize on the potential thermal benefits.

One noteworthy aspect concerning the temperature in salt pillars is that the maximum anomaly is attained at the top of the salt pillar. However, not all salt pillars extend to the same heights, resulting in different temperatures at their respective top. To maximize the chimney effect of salt pillars, drillings need to be precisely at the top of the salt pillars, each having its distinct temperature profile. In the case of the Onstwedde salt pillar, the most efficient drillings would yield thermal energy at approximately 45 °C.

When salt pillars approach the surface, the thickness of the layers above them decreases. These overlying layers typically possess lower thermal conductivity and function as a cap, retaining heat at the top of the pillar. If the cap on top of the salt pillar is thinner, heat retention is reduced, resulting in a lower anomaly at the salt pillar. This variation in cap thickness could significantly impact temperatures, implying that salt pillars closer to the surface may have less potential to harness the geothermal effects efficiently.

5.3 Heat flow due to fluid transport in the rocks

The fluids within the surrounding rocks may potentially undergo convection-like flow, where, in theory, cool water descends at one end of the cell while warm water ascends at the other end. This phenomenon could have a significant impact on subsurface temperatures, resulting in some locations exhibiting much higher or lower temperatures than initially anticipated. Salt pillars or other salt structures might even act as barriers delineating the boundaries of such convection cells. Consequently, at the edges of a salt pillar, the subsurface temperatures could vary significantly, depending on the direction of the convection.

5.4 Future research

To substantiate these theoretical notions, further research is necessary on the convective flow of fluids in the subsurface and the specific conditions under which this occurs. Subsequent investigations can delve into understanding how salt structures influence these convection cells and the resultant effects on subsurface temperatures.

6 Conclusion

In conclusion, this research has provided valuable insights into the thermal behavior of salt pillars and its implications for geothermal energy exploration. The models consistently demonstrate a lateral positive temperature anomaly at the top of salt pillars, with the potential for temperatures up to 20 °C higher than the surrounding subsurface. This suggests that drilling on top of a salt pillar may allow for achieving desired temperatures with shallower and, consequently, more cost-effective boreholes.

The model results show that the presence of the Peelo glacier channel above the salt pillar acts as a thermal insulator, influencing heat retention at the pillar's summit. Additionally, variations in thermal conductivity of overlying layers and different lower boundary conditions produced nuanced effects.

Furthermore, the study raises intriguing possibilities for utilizing geothermal energy from salt pillars, particularly in regions like Groningen, Netherlands, where salt structures are prevalent. The potential for providing thermal heat to cities and villages situated above salt pillars presents an exciting avenue for sustainable energy use.

However, uncertainties remain, especially concerning lower boundary conditions and the influence of convection in surrounding rocks. Further research is essential to refine our understanding of these factors and their impact on subsurface temperatures. Additionally, investigating the convective flow of fluids in the subsurface and how salt structures may influence these processes would contribute to a more comprehensive understanding of geothermal dynamics.

In summary, the findings suggest that salt pillars hold promising potential for geothermal energy extraction, and future research endeavors can play a pivotal role in unlocking the full benefits of this sustainable energy source.

7 Acknowledgements

I am deeply thankful to the following individuals and organizations for their invaluable support to this work:

- My primary supervisor, Fred Beekman, for their continuous guidance, expertise, and unwavering support.
- My co-supervisor, Hans Veldkamp, for their valuable insights, constructive feedback, and encouragement throughout the research process.
- The TNO for providing financial support, enabling the successful completion of this project.
- People working at TNO for helping with the process and their support.
- My intern colleagues and friends for their camaraderie, stimulating discussions, and shared experiences during this research journey.

I express my deepest gratitude to all those who have been part of this endeavor.

References

[1] Damien Bonté et al. "Subsurface temperature of the onshore Netherlands: new temperature dataset and modelling". In: *Netherlands Journal of Geosciences* 91.4 (2012), pp. 491–515.

[2] U Burkitov et al. "Groningen Field Review 2015 Subsurface Dynamic Modelling Report". In: *Report No. EP201603238100, Assen: NAM* (2016).

[3] Alexandros Daniilidis and Rien Herber. "Salt intrusions providing a new geothermal exploration target for higher energy recovery at shallower depths". In: *Energy* 118 (2017), pp. 658–670.

[4] Thomas Hantschel and Armin I Kauerauf. *Fundamentals of basin and petroleum systems modeling*. Springer Science & Business Media, 2009.

[5] Henk Kombrink. *Ondergrondmodellen*. Geraadpleegd op 30-11-2023. Geoexpro. 2022. URL: %5Chref%7BGeoexpro%7D%7Bhttps://geoexpro.com/drilling-into-the-top-of-a-salt-dome-results-in-unexpected-temperatures/%7D.

[6] Quirijn Hoelen et al. "gas storage in salt caverns "aardgasbuffer Zuidwending" The Netherlands". In: *23rd World Gas Conference, Amsterdam*. 2006, p. 6.

[7] Sjoerd J Kluiving et al. "Onshore and offshore seismic and lithostratigraphic analysis of a deeply incised Quaternary buried valley system in the Northern Netherlands". In: *Journal of Applied Geophysics* 53.4 (2003), pp. 249–271.

[8] Xianglan Li et al. "Thermal Properties of Evaporitic Rocks and their Geothermal Effects on the Kuqa Foreland Basin, Northwest China". In: *Geothermics* 88 (2020), p. 101898.

[9] Jacek Majorowicz and Vasile Minea. "Geothermal anomalies in the Gaspésie Peninsula and Madeleine Islands, Québec". In: *GRC Trans* 37 (2013), pp. 295–300.

[10] Volker Manhenke and Horst Beer. "Karten der Erdwärme des Landes Brandenburg". In: ().

[11] TNO - Geologische Dienst Nederland. *Formatie van Peelo*. Geraadpleegd op 12-12-2023. 2023. URL: https://www.dinoloket.nl/stratigrafische-nomenclator/formatie-van-peelo.

[12] NLOG - Netherlands Petroleum Data Management. *NLOG DGM Diep-v4*. Geraadpleegd op 12-12-2023. 2023. URL: https://www.nlog.nl/node/470.

[13] NLOG - Netherlands Petroleum Data Management. *R10558 Velmod-4 NAM Final Public Report*. Accessed on 12-12-2023. 2022. URL: https://www.nlog.nl/sites/default/files/2022-03/r10558_velmod-4_nam_final_public_report.pdf.

[14] K Petersen and I Lerche. "Temperature dependence of thermal anomalies near evolving salt structures: importance for reducing exploration risk". In: *Geological Society, London, Special Publications* 100.1 (1996), pp. 275–290.

[15] Jasmin Raymond et al. "Temperature dependence of rock salt thermal conductivity: Implications for geothermal exploration". In: *Renewable Energy* 184 (2022), pp. 26–35.

[16] Eugene C Robertson. "Thermal properties of rocks". In: (1988).

[17] Stuart J Self et al. "Geothermal heat pump systems: Status review and comparison with other heating options". In: *Applied energy* 101 (2013), pp. 341–348.

[18] TNO-GDN. *Ondergrondmodellen*. Geraadpleegd op 16-10-2023. TNO – Geologische Dienst Nederland. 2023. URL: %5Chref%7BDINOLoket%7D%7Bhttps://www.dinoloket.nl/ondergrondmodellen/kaart%7D.

[19] Alexander Urquhart and Stephen Bauer. "Experimental determination of single-crystal halite thermal conductivity, diffusivity and specific heat from- 75° C to 300° C". In: *International Journal of Rock Mechanics and Mining Sciences* 78 (2015), pp. 350–352.

[20] Heijn Van Gent et al. "The internal geometry of salt structures–a first look using 3D seismic data from the Zechstein of the Netherlands". In: *Journal of Structural Geology* 33.3 (2011), pp. 292–311.

[21] Z Yu et al. "Thermal impact of salt: Simulation of thermal anomalies in the Gulf of Mexico". In: *Pure and Applied Geophysics* 138 (1992), pp. 181–192.